



## FULL LENGTH ARTICLE

# Single-cell transcriptomic analysis reveals transcript enrichment in oxidative phosphorylation, fluid shear stress, and inflammatory pathways in obesity-related glomerulopathy

Yinyin Chen <sup>a</sup>, Yushun Gong <sup>a</sup>, Jia Zou <sup>a</sup>, Guoli Li <sup>a</sup>, Fan Zhang <sup>a</sup>,  
Yiya Yang <sup>a</sup>, Yumei Liang <sup>a</sup>, Wenni Dai <sup>b</sup>, Liyu He <sup>b,\*</sup>,  
Hengcheng Lu <sup>b,c,\*\*,1</sup>

<sup>a</sup> Department of Nephrology, Hunan Provincial People's Hospital, The First Affiliated Hospital of Hunan Normal University, Hunan Clinical Research Center for Chronic Kidney Disease, Changsha, Hunan 410000, China

<sup>b</sup> Department of Nephrology, The Second Xiangya Hospital of Central South University, Hunan Key Laboratory of Kidney Disease and Blood Purification, Changsha, Hunan 410011, China

<sup>c</sup> Cardiovascular Research Institute of Jiangxi Province, Jiangxi Provincial People's Hospital, The First Affiliated Hospital of Nanchang Medical College, Nanchang, Jiangxi 330006, China

Received 16 November 2022; received in revised form 20 June 2023; accepted 24 July 2023

Available online 14 September 2023

## KEYWORDS

Fluid shear stress;  
Inflammation;  
Obesity-related  
glomerulopathy;  
Oxidative  
phosphorylation;  
Single-cell RNA seq

**Abstract** Obesity-related glomerulopathy (ORG) is an independent risk factor for chronic kidney disease and even progression to end-stage renal disease. Efforts have been undertaken to elucidate the mechanisms underlying the development of ORG and substantial advances have been made in the treatment of ORG, but relatively little is known about cell-specific changes in gene expression. To define the transcriptomic landscape at single-cell resolution, we analyzed kidney samples from four patients with ORG and three obese control subjects without kidney disease using single-cell RNA sequencing. We report for the first time that immune cells, including T cells and B cells, are decreased in ORG patients. Further analysis indicated that SPP1 was significantly up-regulated in T cells and B cells. This gene is related to inflammation and cell proliferation. Analysis of differential gene expression in glomerular cells (endothelial

\* Corresponding author.

\*\* Corresponding author. Department of Nephrology, The Second Xiangya Hospital of Central South University, Hunan Key Laboratory of Kidney Disease and Blood Purification, Changsha, Hunan 410011, China.

E-mail addresses: [heliyu1124@csu.edu.cn](mailto:heliyu1124@csu.edu.cn) (L. He), [hengchenglu@163.com](mailto:hengchenglu@163.com) (H. Lu).

Peer review under responsibility of Chongqing Medical University.

<sup>1</sup> These authors contributed equally to this work.

cells, mesangial cells, and podocytes) showed that these cell types were mainly enriched in genes related to oxidative phosphorylation, cell adhesion, thermogenesis, and inflammatory pathways (PI3K-Akt signaling, MAPK signaling). Furthermore, we found that the podocytes of ORG patients were enriched in genes related to the fluid shear stress pathway. Moreover, an evaluation of cell-cell communications revealed that there were interactions between glomerular parietal epithelial cells and other cells in ORG patients, with major interactions between parietal epithelial cells and podocytes. Altogether, our identification of molecular events, cell types, and differentially expressed genes may facilitate the development of new preventive or therapeutic approaches for ORG.

© 2023 The Authors. Publishing services by Elsevier B.V. on behalf of KeAi Communications Co., Ltd. This is an open access article under the CC BY-NC-ND license (<http://creativecommons.org/licenses/by-nc-nd/4.0/>).

## Introduction

The rapid increase in the prevalence of obesity worldwide has led to an increase in obesity-related glomerulopathy, which is characterized by glomerular hypertrophy and focal and segmental glomerulosclerosis in patients with a body mass index  $\geq 30$  kg/m<sup>2</sup> (or  $> 28$  kg/m<sup>2</sup> in the Chinese population).<sup>1–3</sup> Histological signs of obesity-related glomerulopathy include glomerulomegaly, segmental sclerosis,<sup>3–5</sup> interstitial fibrosis, and tubular atrophy,<sup>6</sup> with some cases showing foot effacement and lipid vacuoles in proximal tubular epithelial cells, podocytes, and mesangial cells.<sup>7,8</sup> Efforts are underway to develop better biomarkers for this disease. The National Health and Nutrition Examination Survey reported that abdominal obesity is independently associated with albuminuria even in patients with normal blood pressure and without hyperglycemia.<sup>9</sup> Obesity, or the conditions leading to it, may cause early renal functional and morphological alterations, which increase the risk of chronic kidney disease and end-stage renal disease.<sup>10,11</sup>

At present, the mechanisms underlying the development of obesity-related glomerulopathy (ORG) are thought to include renal hyperfiltration, renin-angiotensin-aldosterone system overactivation, ectopic lipid accumulation, insulin resistance, inflammation, and oxidative stress.<sup>4,5</sup> However, there is a lack of knowledge regarding the cell types and molecular pathways involved in the development and progression of the disease.

Previous studies have identified several important transcriptional alterations in human obesity-related kidney disease using bulk RNA-seq, but these findings are limited by the fact that they represent the average gene expression measured in multiple cell types. The advent of scRNA-seq has made it possible to analyze cell populations at the single-cell level, making it possible to identify changes that occur in each cell type. To shed light on the complexity of obesity-related glomerulopathy, we analyzed different cell types from patients with ORG and matched healthy adult kidneys from obese patients at the single-cell resolution.

Here, we provide a comprehensive catalog of cell types and gene expression at the single-cell level. By characterizing the molecular functions of the differentially expressed genes, we were able to obtain insights into the

development of ORG. The present findings might permit an earlier diagnosis of this disease or its progression and may help identify signaling pathways amenable to early intervention.

## Methods

### Sample collection

#### Sample preparation and tissue procurement

Kidney tissue samples were collected from four patients confirmed to have clinical and pathological evidence of obesity-related glomerulopathy. Control kidney tissues were harvested from three obese patients who had been diagnosed with urinary stones or renal tumors. All tissues were stored and transported on ice at all times until tissue dissociation or freezing. Only minor renal biopsy samples were used for the scRNA-seq procedure.

#### Tissue dissociation and preparation of single-cell preparations

Human kidney tissue samples were immediately transferred to a sterile RNase-free culture dish containing calcium-free and magnesium-free  $1 \times$  PBS on ice. They were then cut into  $0.5 \text{ mm}^2$  pieces and washed with  $1 \times$  PBS to remove the blood and fatty layers.

The washed pieces of tissues were placed in a dissociation solution and incubated at  $37^\circ\text{C}$  in a water bath for 20 min with shaking at 100 rpm. Subsequently, the dissociation was terminated by adding  $1 \times$  PBS containing 10% fetal bovine serum (FBS, V/V) and pipetting up and down 5–10 times to disperse the cells.

The resulting cell suspension was filtered through a  $70\text{--}30 \text{ }\mu\text{m}$  stacked cell strainer, followed by centrifugation at  $300g$  at  $4^\circ\text{C}$  for 5 min. The cell precipitate was resuspended in  $100 \text{ mL}$  of  $1 \times$  PBS (0.04% BSA) and then  $1 \times$  blood cell lysis buffer (MACS 130-094-183,  $10 \times$ ) was added, followed by incubation at room temperature or on ice for 2–10 min. After lysis, the suspension was centrifuged again at  $300 g$  for 5 min. The suspension was resuspended in  $100 \text{ mL}$  of Dead Cell Removal MicroBeads (MACS 130-090-101) and dead cells were removed using the Miltenyi® Dead Cell Removal Kit (MACS 130-090-101). The suspension was resuspended in  $1 \times$  PBS (0.04% BSA) and centrifuged at

300 g at 4 °C for 3 min (repeated twice). The cell suspension was resuspended in 50 mL of 1 × PBS (0.04% BSA). The cell viability was counted by trypan blue exclusion. Only suspensions with viability < 85% were used for gene analyses.

#### Chromium 10x genomics library and sequencing

The final single-cell suspensions were loaded into the 10x chromium instrument, and cell capture (8000 target cells for each sample), cDNA amplification, and library construction were performed according to the manufacturer's instructions for the library construction kit (10X Genomics Chromium Single-Cell 3' kit, V3). After library construction, the NovaSeq 6000 sequencing platform was used for sequencing (paired-end multiplexing run, 150 bp), and the sequencing depth required was 20,000 reads per cell. The above technology was provided by LC-BioTechnology Co. Ltd. (Hangzhou, China).

#### Unsupervised clustering and cell type identification

After filtering the quality of cells (less than 200 or greater than 2500 used to identify unique genes and greater than 5% set as the required percentage of mitochondrial genome content), the expression was homogenized using the Log-Normalize method of the "Normalization" function of Seurat software.

The variables were reduced and then the homogenized expression values were analyzed by principal component analysis. A clustering analysis was performed with Seurat package procedures with a resolution of 1.2. Finally, the identified clusters were visualized using t-distributed Stochastic Neighbor Embedding (tSNE) of the principal components in Seurat.

#### Analysis of marker genes for different cell types

Average gene expression matrices were retrieved for each cluster, differential expression among clusters was identified, and the top markers for each cluster were determined at a high level using the FindAllMarkers implemented function (parameters: only.pos = FALSE, min.pct = 0.2, thresh. use = 0.2).

#### Ligand-receptor interaction analysis

We assigned a probability value to each putative ligand-receptor interaction and performed a substitution test to infer cell-cell communication in a biological sense via Cellphone DB.

#### Real-time quantitative PCR

Gene expression changes identified by scRNA-seq were validated using real-time quantitative PCR (RT-qPCR). Total RNA was isolated from the homogenized whole-kidney lysates. After RNA was obtained, its purity and concentration were analyzed using a Nanodrop 1000 spectrophotometer (Thermo Fisher, USA). The cDNA was synthesized with a high-capacity cDNA reverse transcription kit (Life Tec, America). The primers for genes were as follows: IGFBP-7: 5'-CGAGCAAGGTCCTTCCATAGT-3' (forward); IGFBP-7: 5'-GGTGTCCGGGATCCGATGAC-3' (reverse); MMP-7: 5'-GAGTGAGCTACAGTGGGAACA-3' (forward); MMP-7: 5'-CTATGACGCGGGAGTTTAACAT-3' (reverse); VCAM-1: 5'-GGGAAGATGGTCGTGATCCTT-3' (forward); VCAM-1: 5'-TCTGGGGTGGTCTCGATTTTA-3' (reverse); CCL2: 5'-CAGCCAGATGCAAT

CAATGCC-3' (forward); CCL2: 5'-TGGAACTCCTGAACCCACTTCT-3' (reverse).

#### Western blotting

We validated the changes in RNA expression detected by the scRNA-seq by Western blotting. The Western blot results were verified in seven samples. The human normal (obese) kidney and ORG tissues were lysed with RIPA lysis buffer containing both protease inhibitor and phosphatase inhibitor on ice. Protein lysates were separated by SDS-PAGE and transferred onto a polyvinylidene difluoride membrane. The following primary antibodies were incubated at 4 °C overnight: GAPDH (1:5000, Abcam), VCAM-1 (1:1000, Abcam), MMP-7 (1:2000, Genetex), IGFBP7 (1:5000, Abcam). The second antibody was incubated at room temperature for 2 h. The blots' signal was visualized by using the enhanced chemiluminescence system.

#### Histology

Kidney tissues were fixed in formalin and embedded in paraffin. Then, 4- $\mu$ m kidney sections were cut and stained with hematoxylin and eosin (HE).

#### Comparison of the present scRNA-Seq data with data from a previous study

A previous study obtained scRNA-Seq data for normal kidneys (GSE152938). We compared our current data with these findings, and the results are shown in [Figure S1](#).

#### Statistical analysis

The results were analyzed using SPSS 16.0 and GraphPad Prism 6.0 software. Statistical analyses were performed with Student's *t*-tests and Mann-Whitney *U*-tests to examine the statistical significance of differences, and all data were presented as mean  $\pm$  standard deviation.

## Results

We obtained four renal biopsy samples from patients with ORG, and three samples from obese patients with renal tumors who did not have ORG. The kidney specimens ( $n = 3$ ) from obese patients were obtained after unilateral nephrectomy. These samples were at least 2 cm away from the tumor edge and were proven to be normal renal tissue based on a pathology examination ([Fig. S2](#)). The patients with ORG aged from 27 to 50 years old. All four ORG patients had proteinuria, which ranged from 1.1 to 2.3 g per 24 h. The estimated glomerular filtration rate of the ORG patients ranged from 105 to 120.5 mL/min/1.73 m<sup>2</sup> (mean: 114.25  $\pm$  6.57 mL/min/1.73 m<sup>2</sup>). Additionally, none of the ORG patients had primary renal diseases such as IgA nephropathy, membrane nephropathy, or other secondary factors that might contribute to an increased glomerular volume or focal segmental glomerulosclerosis, such as diabetic nephropathy. Although the two ORG patients combined with hypertension, we found no hypertensive renal arteriolar sclerosis damage on kidney biopsy and no hypertensive retinopathy. The average age of the three obese subjects with cancer was 38.33  $\pm$  11.59 years. Renal tissue pathological examination showed that the mean glomerular diameter in the ORG model groups was

significantly longer than that in the control groups. The kidney pathology of the ORG patients is shown in [Figure S3](#). Additional details for the patients in the ORG and control (obese) subjects are shown in [Table S1](#).

### Single-cell clustering and cell type identification

After filtering out the cells with  $< 200$  genes and  $> 10\%$  mitochondrial genes, a total of 30,810 cells were collected and sequenced from seven samples (representing four ORG patients). Twenty-two distinct cell clusters were defined using an unsupervised clustering analysis and were labeled based on previously characterized lineage-specific markers ([Fig. 1A](#)). The enrichment of different cell clusters in each subject was then calculated ([Fig. 1B](#)). The frequency of cell clusters in the kidney of each subject is represented with bar plots ([Fig. 1C](#)). After calculating the cell proportions of the seven samples ([Fig. 1D](#)), it was noted that there were decreased immune cell clusters (B cells and T cells) and increased cell clusters (endothelial, tubule, and glomerular parietal epithelial cells) in the ORG samples compared with the three control samples. The expression of the top 10 marker genes for each cell population across the 22 clusters is shown in [Figure 1E](#).

### Identification of gene expression changes in the glomerulus of subjects with ORG

We next identified the transcriptomes of the glomerulus in ORG patients and controls. There was no significant difference in the number of podocytes between the ORG (mean =  $30.75 \pm 11.84$ ) and control ( $134.3 \pm 129.8$ ,  $P = 0.3878$ ) samples, although a previous study showed a decreased number of podocytes in ORG patients.<sup>2</sup> The low sample number and cells captured by the instrument may explain the insignificant difference. The differentially expressed genes (DEGs) in podocytes and mesangial and endothelial cells were compared between the ORG and control subject transcripts, as shown in [Figure 2A](#). Several of the genes overexpressed in ORG podocytes (TPM1, CTSC/cathepsin C, PCP4, and KRT19) are reported here for the first time. TPM1, tropomyosin 1, encodes structural proteins important for muscle function and is associated with cardiomyopathy caused by obesity, leading to dilated cardiomyopathy with impaired contractility and diastolic function.<sup>12</sup> Cathepsin, a regulator of inflammatory responses, plays a role in podocyte injury in patients with diabetes<sup>13</sup> and is associated with the glomerular extracellular matrix composition in patients with collapsing focal segmental glomerulosclerosis.<sup>14</sup> ADAMTS1 is a marker of activation in kidney pericytes.<sup>15</sup> A recent study showed that excessive activation of ADAMTS1 contributes to renal fibrosis in hypertensive renal disease and glomerulosclerosis.<sup>16</sup> The expression of ADAMTS1 was similarly increased in the podocytes of subjects with ORG. However, a more in-depth analysis is needed to examine the role(s) of ADAMTS1 in ORG disease.

A KEGG enrichment analysis showed that the DEGs in the podocytes were enriched for biological processes including fluid shear stress, atherosclerosis, and focal adhesion ([Fig. 2B](#)). To confirm the involvement of podocyte failure

and mechanical strain leading to glomerulosclerosis and proteinuria in ORG kidneys, we then analyzed specific kidney cell subsets by combining our data from ORG kidneys with published data from normal subjects. The KEGG analysis showed that the DEGs of podocytes in the patients with ORG were enriched in cell adhesion molecules and cellular senescence pathways ([Table S2](#)). These findings may be associated with individual podocyte shedding and failure, leading to localized glomerular basement membrane shedding, subsequent adhesions to the Bowman capsule, and parietal cell coverage, thus resulting in the development of segmental sclerosis.<sup>4</sup>

A total of 307 mesangial cells were present in the samples from subjects with ORG, and KEGG enrichment for biologic processes ([Fig. 2C](#)) showed that various processes, including phosphorylation, Human T-cell leukemia and virus 1 infection, focal adhesion, thermogenesis, and signaling pathways (PI3K-Akt signaling and MAPK signaling) were enriched ([Table S3](#)). As shown in [Figure 2A](#), the mesangial cells from subjects with ORG had increased expression of IL-1RL1, also named IL33R, which is a member of the interleukin 1 receptor family and results in the production and release of pro-inflammatory cytokines.<sup>17</sup> We also found that the expression of GATA3, a transcription factor overexpressed in obese individuals,<sup>18</sup> was elevated in the mesangial cells of subjects with ORG. As an anti-adipogenic and inflammatory transcription factor, GATA3 inhibits adipogenesis, increases inflammation, and promotes obesity-associated insulin resistance and type 2 diabetes.<sup>19</sup> The high expression of these two genes suggests that chronic inflammation plays a role in the development of ORG.<sup>4</sup>

As shown in [Figure 2D](#), glomerular endothelial cells from subjects with ORG had increased expression of lectin complement components and angiogenic factors (FCN3), regulators of fibrosis and inflammation (S100A4),<sup>20</sup> a water channel protein (AQP1), and a urea transport protein (SLC14A1). The presence of a fibrotic and inflammatory signature in endothelial cells is consistent with prior reports in samples from patients with obesity-related kidney diseases. We herein describe for the first time that S100A4 is increased in the glomerular cells of ORG patients, and is related to endothelial-to-mesenchymal transition. The expression of FABP5, which is involved in endothelial cell proliferation, migration, and lipid metabolism, was also increased. A KEGG pathway enrichment analysis indicated that there was enrichment in pathways involved in inflammation (PI3K-Akt signaling, MAPK signaling), fibrosis (TNF-signaling), focal adhesion, thermogenesis, and oxidative phosphorylation ([Table S4](#)).

We noticed that ORG caused an elevation of inflammatory cytokines ([Table S5](#)), such as vascular cell adhesion molecule (VCAM-1) and C-C motif chemokine ligand 2 (CCL2) which are associated with endothelial cell activation and atherosclerosis in obese patients. It has been shown CCL2 was highly expressed in podocytes stimulated by hyperglycemia, which triggered VCAM-1 up-regulation in glomerular endothelial leading to pro-inflammatory cytokine production, resulting in diabetic glomerulosclerosis.<sup>21</sup> Furthermore, Western blotting and qPCR verified that CCL2 and VCAM-1 were highly expressed in the kidney of samples from patients with ORG ([Fig. S4](#)), especially in ORG podocytes. Meanwhile, both CCL2 and VCAM-1 genes were

enriched in inflammation pathways (TNF signaling, IL-17 signaling) and the fluid shear stress process. The above suggests that two factors (CCL2 and VCAM-1) in ORG disease may be involved in the inflammatory cascade response, and it is also possible that high filtration caused by obesity leads to increased expression of two factors, thus triggering more inflammation in ORG diseases.

### Identification of gene expression changes in the kidney T cells of subjects with ORG

There were 1441 T cells identified in the four renal biopsies of ORG patients. Compared with the control group (obese, non-ORG), the number of T cells was substantially reduced in ORG patients. Further analysis of T cells' function revealed that the DEGs in T cells from ORG were enriched in pathways related to inflammation, cellular senescence, and apoptosis. The ORG T cells had increased expression of chemokines, CCL4, and genes related to oxidative phosphorylation (MT-ATP6, MT-ND1, MT-CYB, and MT-CO2) (Fig. 3A). Ribosomal protein S4 Y-linked 1, a ribosome-related gene, was also found in the T cells of subjects with ORG for the first time. In our samples, the expression of ribosomal protein S4 Y-linked 1 was significantly increased in T cells. Ribosomal protein S4 Y-linked 1, also a stress-responsive gene, is involved in cell death and the production of pro-inflammatory cytokines during endothelial dysfunction.<sup>22</sup> Uromodulin is a glycoprotein that is highly expressed in the T cells of ORG patients. Serum uromodulin is a novel tissue-specific biomarker for kidney function, and a low serum uromodulin level may indicate a decreased renal reserve in individuals with metabolic syndrome.<sup>23</sup> The mechanism underlying the increased expression of uromodulin in the T cells of patients with ORG remains unclear.

As shown in Table S6, the DEGs in T cells from ORG patients showed enrichment of genes involved in PI3K-Akt signaling, NF-kappa B signaling, Toll-like receptor signaling, and Th17 cell differentiation. A KEGG pathway enrichment analysis showed oxidative phosphorylation, thermogenesis, cellular senescence, and apoptosis to be altered in the T cells of the ORG patients (Fig. 3B). Furthermore, genes in pathways related to protein binding (biological process) and positive regulation of transcription by RNA polymerase II (biological process) were highly enriched (Fig. 3C). Further studies are required to shed light onto the biological effects and molecular consequences of these changes in T cells in patients with ORG.

### Gene expression changes in the B cells of subjects with ORG

Compared with the control group, the number of B cells was also decreased in ORG patients. Studies have reported that an abundant number of B cells were present in the kidneys of patients with lupus nephritis<sup>24,25</sup> and diabetic kidney diseases,<sup>26,27</sup> which contributed to immune-mediated kidney injury. In addition, B cell dysfunction is related to membranous nephropathy<sup>28</sup> and recurrent focal segmental glomerulosclerosis.<sup>29</sup> In our study, DEGs in B cells from ORG were particularly enriched in processes related to transcription, apoptosis, neutrophil degranulation, and

oxidation-reduction. Although the number of B cells in the ORG groups was lower than in the control groups, B cells in ORG may play an adequate role in the damage of renal parenchymal cells, which may be the initiating factor of inflammation.

As shown in Figure 4A, a cellular component analysis identified several differentially expressed gene sets located in both the nucleus and cytoplasm. Furthermore, genes enriched in molecular functions, such as the binding to proteins, RNA, DNA, and nucleotides, may provide potential therapeutic targets. We also identified altered pathways in the B cells of ORG subjects. Several signaling pathways, including those implicated in ribosome function, Parkinson's disease, thermogenesis, and oxidative phosphorylation were up-regulated (Fig. 4B). As shown in Figure 4C, there was overexpression of several genes (SPP1, MMP7, CCL3, UMOD/uromodulin and IGFBP7) in the B cells of subjects with ORG. Matrix metalloproteinase-7 (MMP-7), a secreted zinc-dependent endopeptidase, is barely expressed in normal adult kidneys but is up-regulated in chronic kidney disease.<sup>30</sup> In glomerular diseases, MMP-7 can trigger podocyte injury and impair the glomerular filtration barrier. As verified in our PCR and Western blotting experiments, MMP7 was highly expressed in the kidney tissue of ORG groups (Fig. S4), which may be a marker in ORG progression.

SPP1, also named osteopontin (OPN), is a secreted, phosphorylated integrin-binding protein<sup>31</sup> with known roles in B-cell development.<sup>32,33</sup> In our study, OPN was found to be one of the most highly up-regulated genes in the kidney B cells from ORG patients compared with controls. The role of CC chemokines (CCL3, CCL4) in human obesity is related to their increasing systemic inflammation.<sup>34</sup> In our study, we found that CCL3, CCL3L1, CCL4, and CCL4L2 were all also increased in the B cells of patients with ORG compared to the control subjects.

We also observed a pronounced elevation of ORG-induced secreted proteins, IGFBPs (insulin-like growth factor-binding proteins), which play critical roles in various metabolic processes. In particular, IGFBP7 expression is higher in obese children than in healthy controls.<sup>35</sup> Moreover, IGFBP-7 levels are associated with insulin resistance and the risk of metabolic syndrome<sup>36</sup> and are also strongly related to body mass index.<sup>37</sup> As shown in Figure S4, RT-PCR and Western blotting analysis revealed that IGFBP7 transcript elevation was accompanied by increased protein expression in ORG kidneys.

### Altered signaling networks in the subjects with ORG

To explore the intercellular signaling alterations present in patients with ORG, potential interactions of receptors and ligands were examined in different cell types of the kidneys from both control and ORG subjects (Fig. 5A, B). We adopted a well-established intercellular communication inference method, CellPhoneDB,<sup>38</sup> to predict cell-cell interactions, which might provide future therapeutic targets for ORG. We identified distinct cell-cell crosstalk in different immune cells between the control and ORG subjects (Fig. 5C, D). CD74, a transmembrane glycoprotein, is expressed on antigen-presenting cells, including dendritic

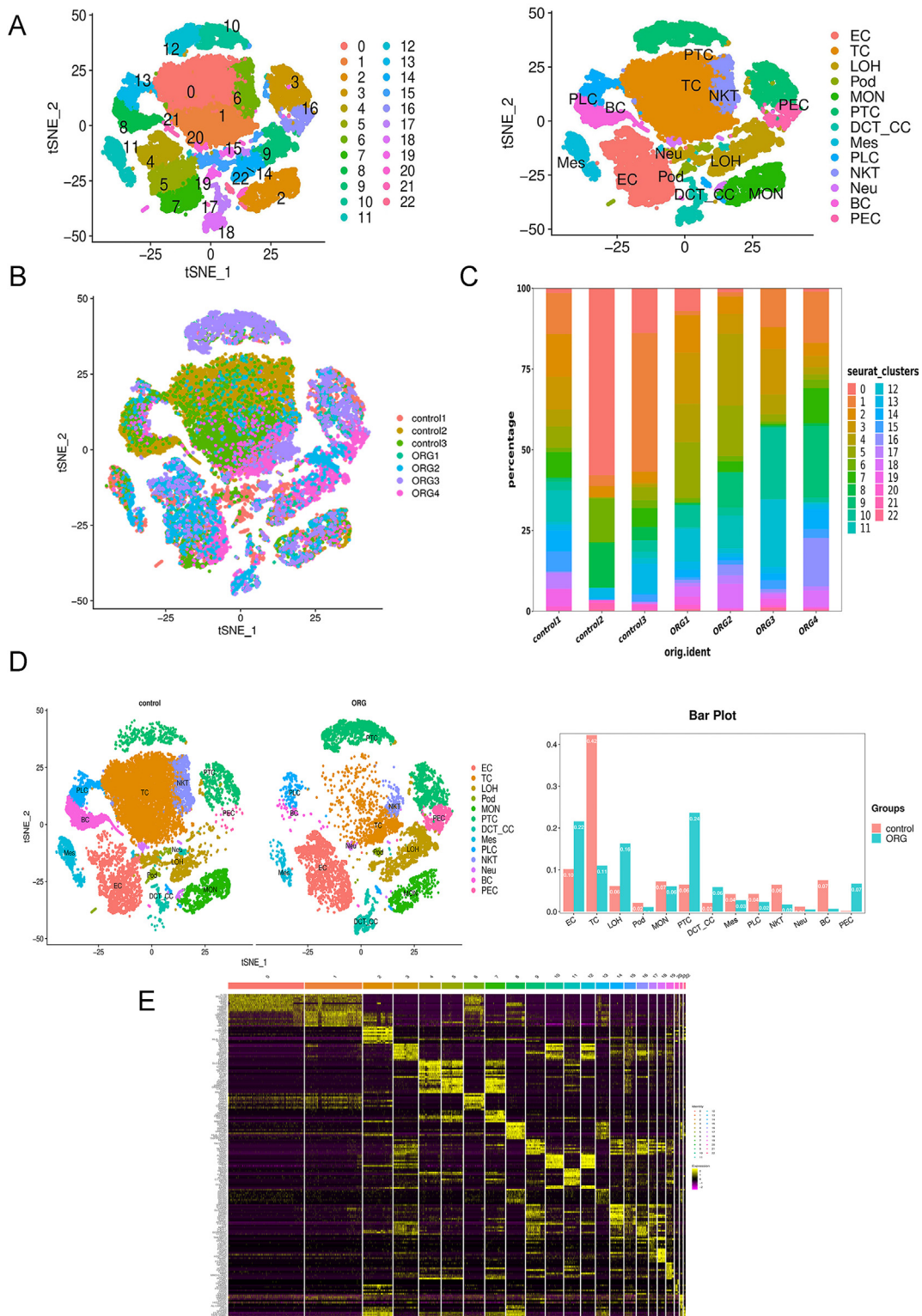


**Figure 1** Cell diversity analysis by single-cell RNA-sequencing in ORG and control (obese, non-ORG) subjects. **(A)** Unsupervised clustering identified 22 distinct cell types, as shown in a t-distributed stochastic neighbor embedding map. Mes, mesangial cell; EC, glomerular endothelial cell; Pod, podocyte; PEC, parietal epithelial cell; PTC, proximal tubule cell; LOH, loop of Henle; DCT\_CC, distal tubule cell\_collecting cell; TC, T cell; BC, B cell; MON, monocyte; PLC, plasma cell; NKT, natural killer T cell; Neu, neutrophil. **(B)** The t-distributed stochastic neighbor embedding analysis of cell clusters from different ORG patients ( $n = 4$ ) and obese control patients ( $n = 3$ ). The color of the cells reflects the individual origin. **(C)** The bar charts showing the frequency of kidney cell clusters in the different subjects. The blocks denote different subjects, and their height is proportional to the number of cells. **(D)** The bar plot showing the proportions of cell clusters in the ORG and control (obese, non-ORG) kidney samples.

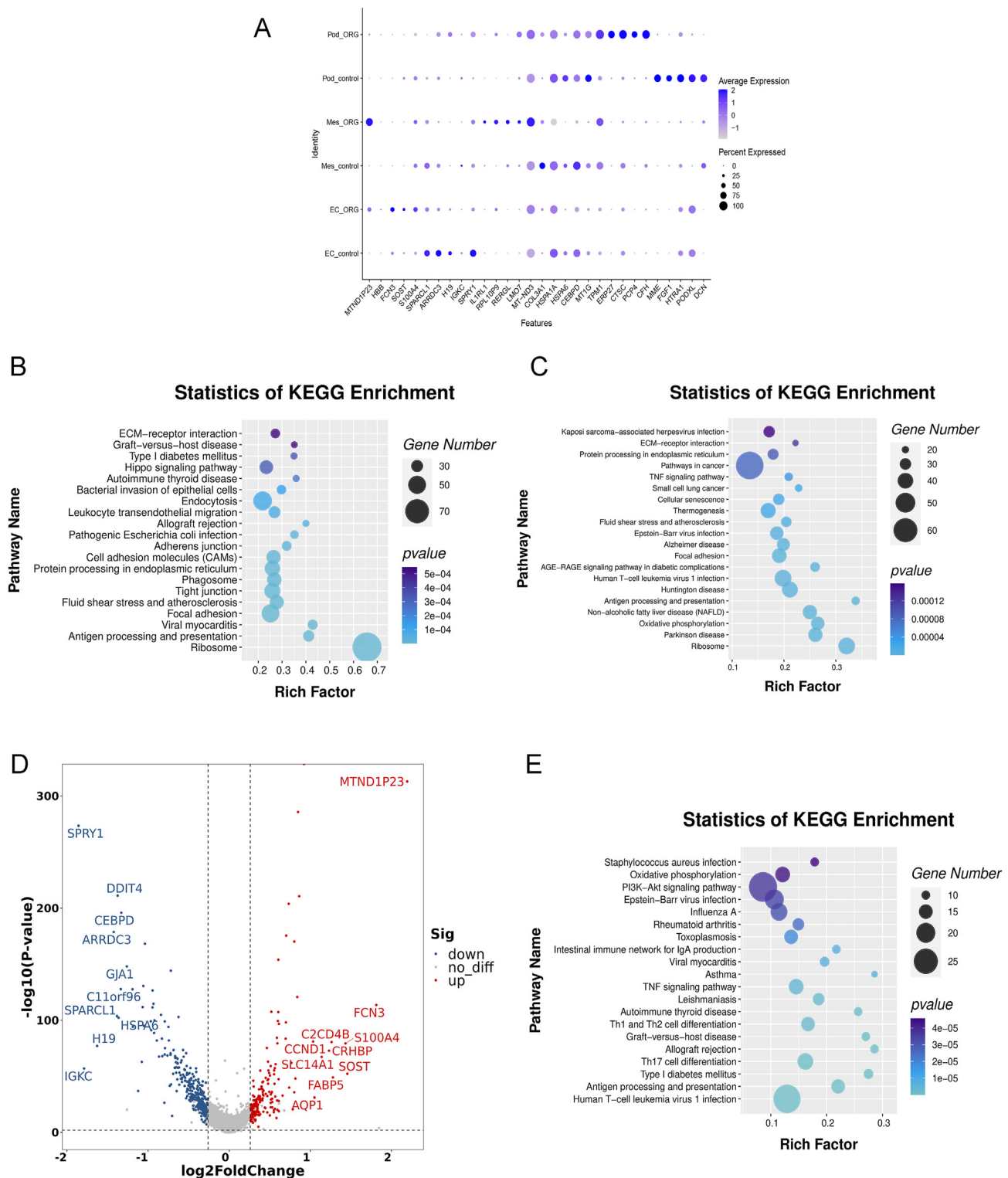


**Figure 2** DEGs and pathways up-regulated in glomerular cells. (A) The transcription profiles of ORG and control cells were compared, and DEGs were found in podocytes, mesangial cells, and endothelial cells. (B) A KEGG enrichment analysis of the DEGs mainly enriched in ORG podocytes. (C) A KEGG enrichment analysis of the DEGs enriched in ORG mesangial cells. (D) A differential gene volcano map of glomerular endothelial cells from ORG and control subjects. (E) The KEGG enrichment analysis of the DEGs mainly enriched in glomerular endothelial cells.

The t-distributed stochastic neighbor embedding analysis of kidney cells showed 13 distinct clusters in the control (left) and ORG (right) patients. (E) Heatmap of the top ten specific marker genes for each cluster of kidney cells.

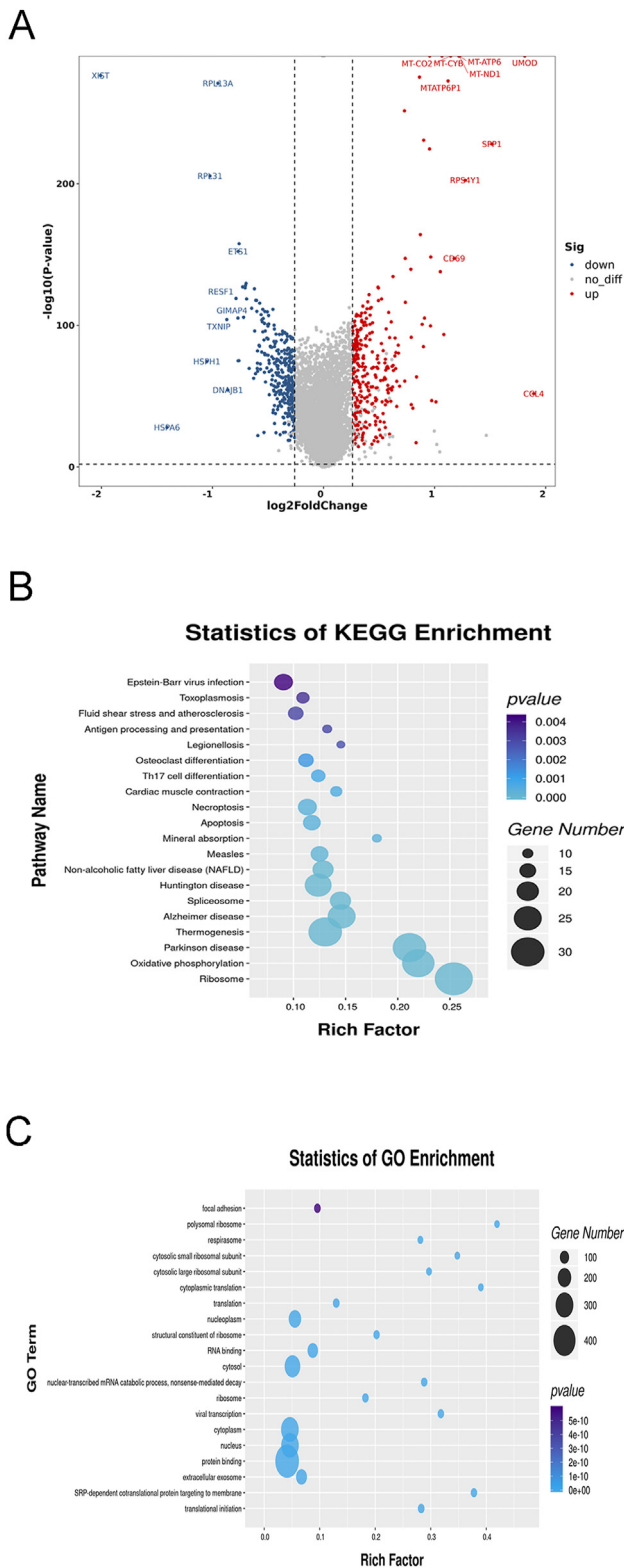


**Figure 3** DEGs and pathway signaling in the T cells from ORG and control subjects. **(A)** Differential gene volcano map of T cells comparing the ORG subjects with the control subjects. **(B, C)** KEGG and GO enrichment analyses revealed the DEGs that were mainly enriched in T cells.

cells, monocytes/macrophages, and B cells.<sup>39</sup> It acts as a cell surface receptor for the cytokine macrophage migration inhibitory factor, which promotes inflammatory responses and contributes to the pathogenesis of obesity and kidney diseases.<sup>40,41</sup> We found that the CD74 expressed by both B cells and monocytes interacted with the migration inhibitory factor expressed in immune cells, including B cells, monocytes, natural-killer T cells, neutrophils, T cells, and plasma cells (Fig. 5C). In addition, we predicted different cell type interactions between control (Fig. S5A) and ORG (Fig. S5B) subjects. Glomerular endothelial cells also expressed CD74 and interacted with podocytes, proximal tubule cells, glomerular parietal epithelial cells, and several immune cells. These results suggest that CD74/migration inhibitory factor may play a role in the pathogenesis of ORG.

An in-depth study was performed for the remaining interactions in ligand-receptor pairs among different cell types. As shown in Figure 5E and F, CellPhoneDB revealed increased interactions between the parietal epithelial cells and the podocytes (Fig. 5F). Similarly, we found that most cell type-specific interaction events in samples from control subjects occurred in tubular cells, while the most interactions in samples from ORG patients occurred in the parietal epithelial cells and podocytes.

## Discussion

Here, we reported the single-cell transcriptome of kidney cells from both control and ORG subjects. We presented a comprehensive scRNA-seq analysis of human renal biopsy tissue from ORG patients. By comparing DEGs in different cell clusters, we observed that there was up-regulation of genes related to oxidative phosphorylation, thermogenesis, and cellular senescence and apoptosis, as well as pathways that are associated with inflammation, TNF signaling, and antigen processing and presentation. Overall, our findings present a panoramic view of the cellular and molecular programs activated in ORG and reveal several novel insights into the pathogenesis of ORG based on findings involving cell type-specific gene expression, cell-cell crosstalk, and signaling pathways.

An increased body mass requires increased blood perfusion through all organs, including the kidneys.<sup>7</sup> Glomerular hyperfiltration will increase shear stress on the podocytes, which leads to glomerular hypertrophy and podocyte detachment and loss.<sup>2,42</sup> In our present study, we found that there was no significant difference in the number of podocytes between the disease and obese control groups. However, a subset of parietal epithelial cells, as podocyte progenitors,<sup>43</sup> was increased in ORG patients. Whether parietal epithelial cell replacement occurs in human beings, and the role those cells play in the response to obesity, need further exploration. Pathways related to fluid shear stress, focal adhesion, and regulation of the actin cytoskeleton were increased in subjects with ORG.

To validate our findings, we downloaded the previously published single-cell kidney data from healthy kidney



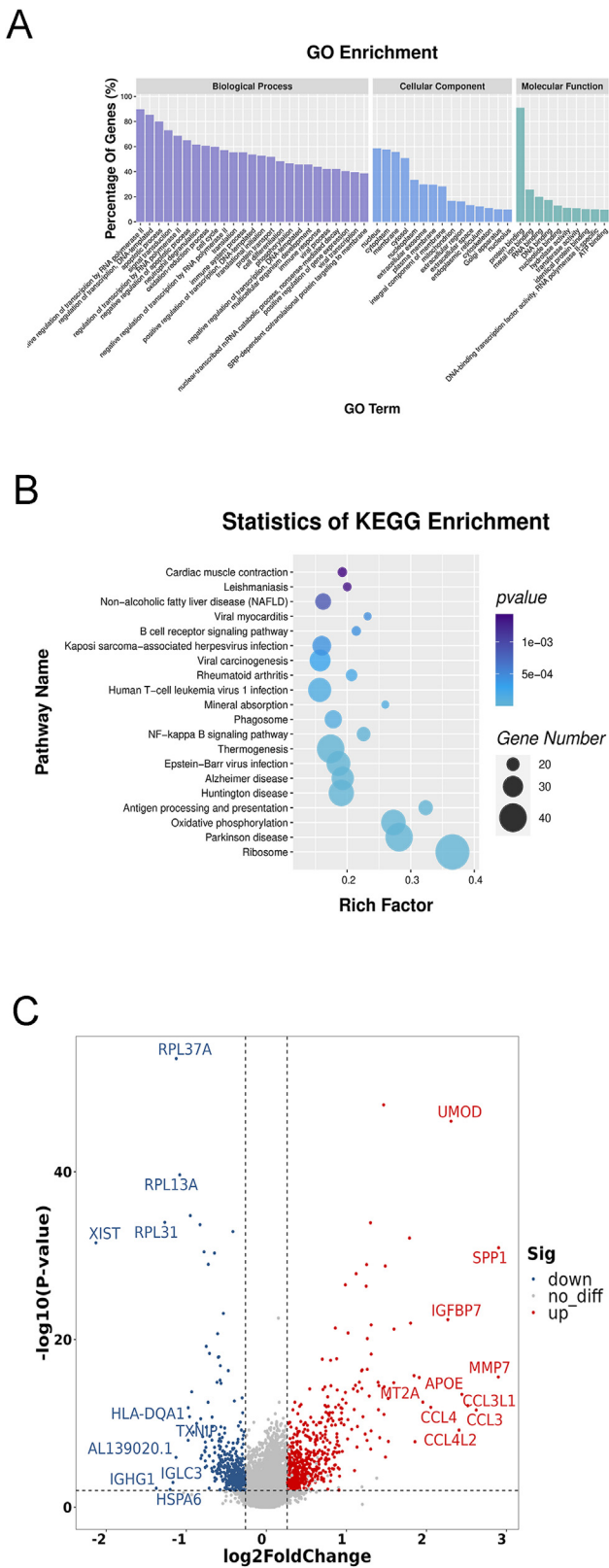


**Figure 4** DEGs and pathway signaling in ORG and obesity B cells. (A, B) A GO and KEGG enrichment analysis revealed the DEGs were mainly enriched in B cells. (C) A differential gene volcano map of B cells comparing the ORG subjects with the control subjects.

subjects. A KEGG enrichment analysis of ORG and healthy controls revealed that the DEGs of podocytes were enriched in cell adhesion molecules and cellular senescence pathways, and the DEGs of glomerular parietal epithelial cells were also enriched in cell adhesion pathways. These findings are similar to our results comparing the ORG subjects with the obese (non-ORG) control subjects. Furthermore, podocin, a protein expressed exclusively by podocytes to perform their functions,<sup>44</sup> was decreased in ORG patients, indicating the presence of podocyte injury induced by hyperfiltration in obese individuals.

Accumulating data suggest that the hyperfiltration in ORG is related to increased susceptibility to oxidant injury, which means that there is likely reactive oxygen species production leading to glomerular endothelial dysfunction and increased inflammatory cytokines.<sup>45–47</sup>

Also, we verified the up-regulation of CCL2 and VCAM-1 genes in ORG kidneys, which could be caused by high filtration in ORG, eventually triggering an inflammatory cascade response. Subsequently, impaired endothelial cell function contributes to podocyte and mesangial injury.<sup>45,48</sup> In our investigation, the pathways up-regulated in endothelial cells were mainly enriched in cell focal adhesion, PI3K-Akt signaling, MAPK signaling, and the TNF signaling pathway. There was also overexpression of genes that regulate angiogenesis (*FCN3*, *FABP5*), insulin resistance (*S100A4*, *SOST*), glycerol metabolism, renal water transport (*AQP1*), and urea transport (*SLC14A1*) found in our study. To our knowledge, most of these findings have not been reported previously in ORG disease. Accordingly, these findings suggest that alterations in the glomerular endothelial cells may play a vital role in the development of ORG. The markers and genes discussed above need to be validated in larger studies, but may be useful as biomarkers for the early detection of the disease, or may represent novel therapeutic targets.

We further predicted cell-cell interaction networks by analyzing ligand-receptor expression. Our data revealed that parietal epithelial cells, glomerular cells (glomerular endothelial cells, mesangial cells, and podocytes), and immune cells all play critical roles in this process. For example, inflammatory and chemokine signaling pathways were observed to be up-regulated in the kidneys of subjects with ORG. We found that B cells, endothelial cells, and monocytes expressed CD74, interacting with their receptor (migration inhibitory factor), in several kidney cell types, including podocytes, immune cells, mesangial cells, proximal tubule cells, and parietal epithelial cells. These interactions are of importance as they may represent novel therapeutic targets.

There were relatively lower numbers of both T and B cells in the ORG kidneys. It is unclear whether the decrease in these cells is due to cell death or that injured cells are more susceptible to loss during enzymatic digestion and dissociation. Further analysis of T cells function revealed that the DEGs in T cells from ORG were enriched in pathways related to inflammation and cellular senescence and apoptosis. At present, the function of T and B cells in ORG is still to be solved. Although they are less numerous in the ORG groups, their roles in renal parenchymal cell injury may be an initiating factor such as inflammation, which activates downstream a series of injuries to renal

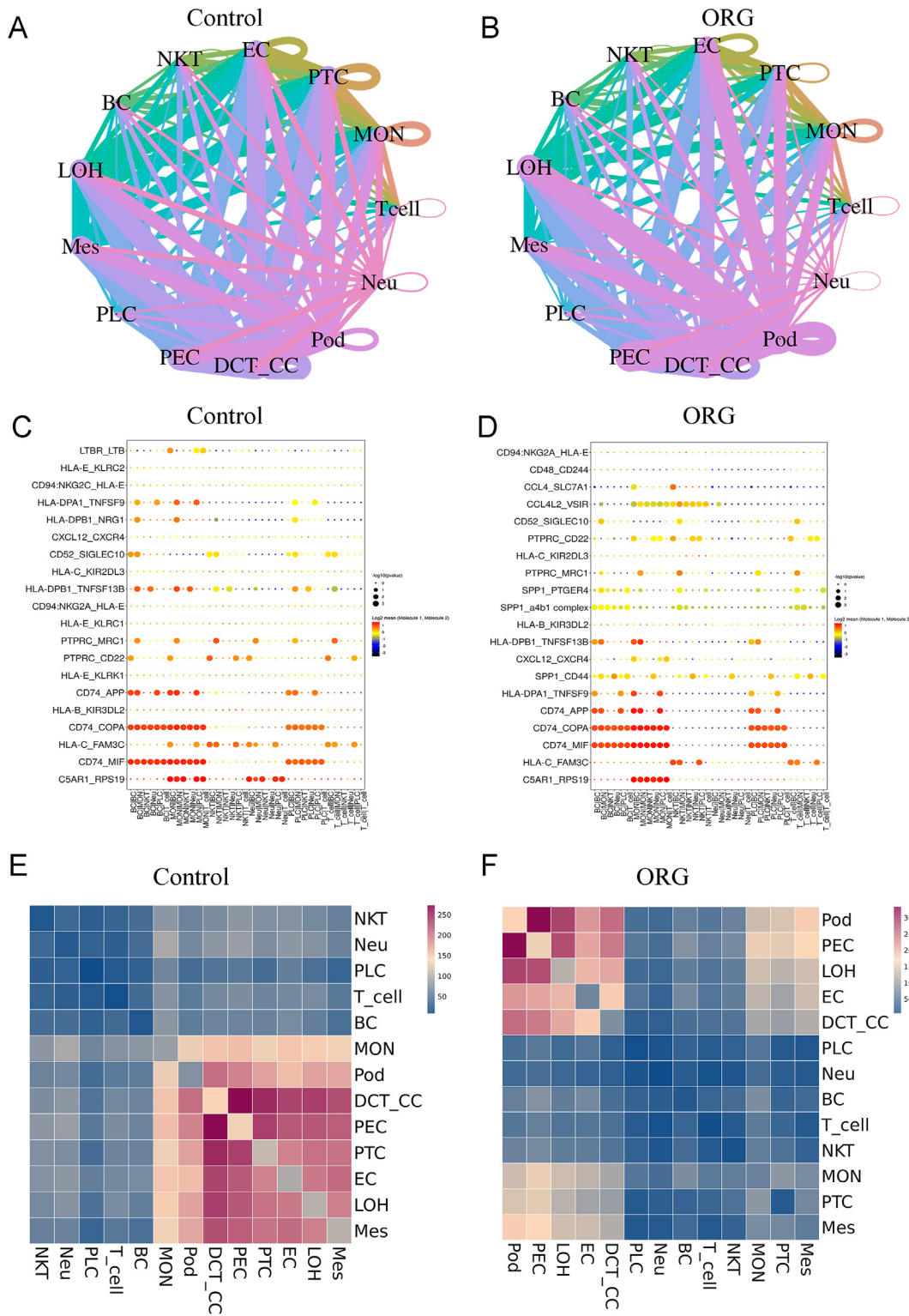


**Figure 5** Cell-cell communication networks and cell type-specific interactions in control and ORG kidney cells identified using CellPhoneDB. (A, B) Visualized network showing the cell-cell interaction events among control (A) and ORG (B) kidney cells. (C, D) Cell type-specific interactions among control (C) and ORG (D) kidney immune cells. (E, F) The heatmaps displaying the interaction events in control (E) and ORG (F) kidney cells.

parenchymal cells, as can be confirmed from our comparative analysis.

There have been two mechanisms identified as underlying OPN-mediated regulation of the B-cell response.<sup>31</sup> In

some infections, IL-4 activates B cell signaling through PI3K and NF-κB to induce OPN secretion, which contributes to the expression of cytokines and chemokines and is strongly associated with autoimmunity.<sup>49</sup> Evidence suggests that

low-grade systemic inflammation plays an important role in ORG, and the OPN in T and B cells was found to be highly expressed in the ORG samples in our present study. Whether this high expression of OPN in B cells and T cells of ORG patients is due to enhanced proliferation or is related to the B cell- and T cell-mediated inflammation needs further exploration. Furthermore, OPN acts as a cytokine and is highly expressed in obesity-induced adipose tissue, resulting in obesity-associated insulin resistance and systemic inflammation.<sup>50</sup> Therefore, it is clinically significant to explore the role of OPN in ORG disease.

Additionally, increased expression of IGFBP7 was found in the B cells of the ORG samples. This gene has previously been used as a biomarker for the early diagnosis and risk stratification of acute kidney injury<sup>51–53</sup> owing to its ability to mark injured tubular epithelium caused by septic and ischemic insults.<sup>54</sup> Upon injury, renal tubular cells enter a short period of G1 cell cycle arrest to protect against kidney injury.<sup>55,56</sup> Future studies could focus on the predictive value of serum IGFBP7 for diagnosing ORG. Further studies are needed to analyze how the different types of immune cells contribute to the progression of ORG.

Our work identified unique cell-specific transcription, as well as several novel genes, signaling pathways, and potential ligand-receptor interactions in subjects with ORG, which could provide a basis for understanding the pathogenesis of ORG. To determine the specificity of the gene expression profiles found in the ORG subjects in our study, we compared them with the changes in glomerular gene expression observed in diabetic mouse models and human subjects.<sup>57</sup> We noted that ORG was associated with the increased expression of genes associated with fluid shear stress, focal adhesion, cellular senescence, and oxidative phosphorylation compared with controls. The gold standard diagnosis of ORG is currently based on biopsy, but there is a higher risk of complications associated with biopsy in these patients due to their obesity. Thus, it is difficult for physicians to diagnose ORG, and the introduction of a non- or minimally-invasive diagnostic process involving urine or venous blood would be ideal. Therefore, early markers of renal injury and potential targets that can be used in the diagnosis and treatment of ORG are urgently needed. Our present scRNA-seq data provide several avenues for future research that might provide such markers.

We recognize that there are limitations regarding this study associated with the relatively small sample size and limited cell capture. We also recognize that there may have been differences in the responses to obesity-induced injury, as well as intrinsic and extrinsic noise, which may have reduced the reliability of the data. Studies with large cohorts and further validation via functional studies *in vitro* and in animal models of ORG will be needed to capture the full picture regarding disease development. However, our data provide interesting insights that might spur such research and could provide potential targets for the diagnosis or treatment of ORG.

## Ethics declaration

This project was approved by the Medical Ethics Committees of the Department of Nephrology, Hunan Provincial

People's Hospital, The First Affiliated Hospital of Hunan Normal University, Changsha, and the Department of Nephrology, The Second Xiangya Hospital of Central South University, Hunan Key Laboratory of Kidney Disease and Blood Purification, Changsha, Hunan. Each patient provided written informed consent and all experiments were conducted according to the study protocol. The study was undertaken with the patient's consent.

## Author contributions

HL and LH conceived the project and designed the study. ZJ, GY, and LG collect the clinical samples and analyzed the clinical data. CY wrote the manuscript. ZF, YY, LY, and DW discussed the results and edited the manuscript. All authors read and approved the final manuscript.

## Conflict of interests

All authors declare that they do not have competing interests.

## Funding

This work was supported by the Hunan Provincial Natural Science Foundation for Outstanding Youth (China) (No. 2022JJ10093, 2020JJ2020), the Scientific Research Fund of Hunan Provincial Health Commission (China) (No. B202303056777), the Major Research and Development Program of Hunan Province, China (No. 2020SK2116), and the Key Program of Hunan Provincial Health Commission (China) (No. 202203052969).

## Data availability

The datasets analyzed during the current study are available from the corresponding author upon reasonable request.

## Acknowledgements

We would like to thank all the participants for donating samples and the support received from the Hunan Provincial Natural Science Foundation for Outstanding Youth, the Scientific Research Fund of Hunan Provincial Health Commission, the Major Research and Development Program of Hunan Province, and the Key Program of Hunan Provincial Health Commission, China.

## Appendix A. Supplementary data

Supplementary data to this article can be found online at <https://doi.org/10.1016/j.gendis.2023.101101>.

## References

1. Tsuboi N, Koike K, Hirano K, Utsunomiya Y, Kawamura T, Hosoya T. Clinical features and long-term renal outcomes of

- Japanese patients with obesity-related glomerulopathy. *Clin Exp Nephrol*. 2013;17(3):379–385.
2. Chen HM, Liu ZH, Zeng CH, Li SJ, Wang QW, Li LS. Podocyte lesions in patients with obesity-related glomerulopathy. *Am J Kidney Dis*. 2006;48(5):772–779.
  3. Kambham N, Markowitz GS, Valeri AM, Lin J, D'Agati VD. Obesity-related glomerulopathy: an emerging epidemic. *Kidney Int*. 2001;59(4):1498–1509.
  4. D'Agati VD, Chagnac A, de Vries AP, et al. Obesity-related glomerulopathy: clinical and pathologic characteristics and pathogenesis. *Nat Rev Nephrol*. 2016;12(8):453–471.
  5. Martínez-Montoro JI, Morales E, Cornejo-Pareja I, Tinahones FJ, Fernández-García JC. Obesity-related glomerulopathy: current approaches and future perspectives. *Obes Rev*. 2022;23(7):e13450.
  6. Serra A, Romero R, Lopez D, et al. Renal injury in the extremely obese patients with normal renal function. *Kidney Int*. 2008;73(8):947–955.
  7. de Vries AP, Ruggenti P, Ruan XZ, et al. Fatty kidney: emerging role of ectopic lipid in obesity-related renal disease. *Lancet Diabetes Endocrinol*. 2014;2(5):417–426.
  8. Bobulescu IA, Lotan Y, Zhang J, et al. Triglycerides in the human kidney cortex: relationship with body size. *PLoS One*. 2014;9(8):e101285.
  9. Sarathy H, Henriquez G, Abramowitz MK, et al. Abdominal obesity, race and chronic kidney disease in young adults: results from NHANES 1999-2010. *PLoS One*. 2016;11(5):e0153588.
  10. Hsu CY, McCulloch CE, Iribarren C, Darbinian J, Go AS. Body mass index and risk for end-stage renal disease. *Ann Intern Med*. 2006;144(1):21–28.
  11. Ejerblad E, Fored CM, Lindblad P, Fryzek J, McLaughlin JK, Nyrén O. Obesity and risk for chronic renal failure. *J Am Soc Nephrol*. 2006;17(6):1695–1702.
  12. Wang F, Li Z, Song T, et al. Proteomics study on the effect of silybin on cardiomyopathy in obese mice. *Sci Rep*. 2021;11(1):7136.
  13. Audzeyenka I, Rachubik P, Rogacka D, et al. Cathepsin C is a novel mediator of podocyte and renal injury induced by hyperglycemia. *Biochim Biophys Acta Mol Cell Res*. 2020;1867(8):118723.
  14. Merchant ML, Barati MT, Caster DJ, et al. Proteomic analysis identifies distinct glomerular extracellular matrix in collapsing focal segmental glomerulosclerosis. *J Am Soc Nephrol*. 2020;31(8):1883–1904.
  15. Schrimpf C, Xin C, Campanholle G, et al. Pericyte TIMP3 and ADAMTS1 modulate vascular stability after kidney injury. *J Am Soc Nephrol*. 2012;23(5):868–883.
  16. Toba H, Ikemoto MJ, Kobara M, Nakata T. Secreted protein acidic and rich in cysteine (SPARC) and a disintegrin and metalloproteinase with thrombospondin type 1 motif (ADAMTS1) increments by the renin-angiotensin system induce renal fibrosis in deoxycorticosterone acetate-salt hypertensive rats. *Eur J Pharmacol*. 2022;914:174681.
  17. Pinto SM, Subbannayya Y, Rex DAB, et al. A network map of IL-33 signaling pathway. *J Cell Commun Signal*. 2018;12(3):615–624.
  18. Al-Jaber H, Al-Mansoori L, Elrayess MA. GATA-3 as a potential therapeutic target for insulin resistance and type 2 diabetes mellitus. *Curr Diabetes Rev*. 2021;17(2):169–179.
  19. Al-Mansoori L, Al-Jaber H, Madani AY, et al. Suppression of GATA-3 increases adipogenesis, reduces inflammation and improves insulin sensitivity in 3T3L-1 preadipocytes. *Cell Signal*. 2020;75:109735.
  20. Li Z, Li Y, Liu S, Qin Z. Extracellular S100A4 as a key player in fibrotic diseases. *J Cell Mol Med*. 2020;24(11):5973–5983.
  21. Alghamdi TA, Batchu SN, Hadden MJ, et al. Histone H3 serine 10 phosphorylation facilitates endothelial activation in diabetic kidney disease. *Diabetes*. 2018;67(12):2668–2681.
  22. Chen Y, Chen Y, Tang C, et al. RPS4Y1 promotes high glucose-induced endothelial cell apoptosis and inflammation by activation of the p38 MAPK signaling. *Diabetes Metab Syndr Obes*. 2021;14:4523–4534.
  23. Then C, Then H, Lechner A, et al. Serum uromodulin is inversely associated with the metabolic syndrome in the KORA F4 study. *Endocr Connect*. 2019;8(10):1363–1371.
  24. Der E, Suryawanshi H, Morozov P, et al. Tubular cell and keratinocyte single-cell transcriptomics applied to lupus nephritis reveal type I IFN and fibrosis relevant pathways. *Nat Immunol*. 2019;20(7):915–927.
  25. Arazi A, Rao DA, Berthier CC, et al. The immune cell landscape in kidneys of patients with lupus nephritis. *Nat Immunol*. 2019;20(7):902–914.
  26. Wei Y, Gao X, Li A, Liang M, Jiang Z. Single-nucleus transcriptomic analysis reveals important cell cross-talk in diabetic kidney disease. *Front Med*. 2021;8:657956.
  27. Wilson PC, Wu H, Kirita Y, et al. The single-cell transcriptomic landscape of early human diabetic nephropathy. *Proc Natl Acad Sci U S A*. 2019;116(39):19619–19625.
  28. Fervenza FC, Appel GB, Barbour SJ, et al. Rituximab or cyclosporine in the treatment of membranous nephropathy. *N Engl J Med*. 2019;381(1):36–46.
  29. Fornoni A, Sageshima J, Wei C, et al. Rituximab targets podocytes in recurrent focal segmental glomerulosclerosis. *Sci Transl Med*. 2011;3(85):e3002231.
  30. Liu Z, Tan RJ, Liu Y. The many faces of matrix metalloproteinase-7 in kidney diseases. *Biomolecules*. 2020;10(6):E960.
  31. Rittling SR, Singh R. Osteopontin in immune-mediated diseases. *J Dent Res*. 2015;94(12):1638–1645.
  32. Lampe MA, Patarca R, Iregui MV, Cantor H. Polyclonal B cell activation by the Eta-1 cytokine and the development of systemic autoimmune disease. *J Immunol*. 1991;147(9):2902–2906.
  33. Leavenworth J, Verbinnen B, Yin J, Huang H, Cantor H. A p85 $\alpha$ -osteopontin axis couples the ICOS receptor to sustained Bcl-6 expression by follicular helper and regulatory T cells. *Nat Immunol*. 2014;16:96–106.
  34. Huber J, Kiefer FW, Zeyda M, et al. CC chemokine and CC chemokine receptor profiles in visceral and subcutaneous adipose tissue are altered in human obesity. *J Clin Endocrinol Metab*. 2008;93(8):3215–3221.
  35. Czogała W, Strojny W, Tomasiak P, et al. The insight into insulin-like growth factors and insulin-like growth-factor-binding proteins and metabolic profile in pediatric obesity. *Nutrients*. 2021;13(7):2432.
  36. Liu Y, Wu M, Ling J, et al. Serum IGFBP7 levels associate with insulin resistance and the risk of metabolic syndrome in a Chinese population. *Sci Rep*. 2015;5:10227.
  37. López-Bermejo A, Khosravi J, Fernández-Real JM, et al. Insulin resistance is associated with increased serum concentration of IGF-binding protein-related protein 1 (IGFBP-rP1/MAC25). *Diabetes*. 2006;55(8):2333–2339.
  38. Vento-Tormo R, Efremova M, Botting RA, et al. Single-cell reconstruction of the early maternal-fetal interface in humans. *Nature*. 2018;563(7731):347–353.
  39. Calandra T, Roger T. Macrophage migration inhibitory factor: a regulator of innate immunity. *Nat Rev Immunol*. 2003;3:791–800.
  40. Bruchfeld A, Wendt M, Miller EJ. Macrophage migration inhibitory factor in clinical kidney disease. *Front Immunol*. 2016;7:8.
  41. Kong YZ, Chen Q, Lan HY. Macrophage migration inhibitory factor (MIF) as a stress molecule in renal inflammation. *Int J Mol Sci*. 2022;23(9):4908.

42. Giannini G, Kopp JB, Rosenberg AZ. Podocytopathy in obesity: challenges of living large. *Semin Nephrol.* 2021;41(4):307–317.
43. Eng DG, Sunseri MW, Kaverina NV, Roeder SS, Pippin JW, Shankland SJ. Glomerular parietal epithelial cells contribute to adult podocyte regeneration in experimental focal segmental glomerulosclerosis. *Kidney Int.* 2015;88(5):999–1012.
44. Gubler MC. Podocyte differentiation and hereditary proteinuria/nephrotic syndromes. *J Am Soc Nephrol.* 2003;14(Suppl 1):S22–S26.
45. Zhang M, Gao X, Wu J, et al. Oxidized high-density lipoprotein enhances inflammatory activity in rat mesangial cells. *Diabetes Metab Res Rev.* 2010;26(6):455–463.
46. Quigley JE, Elmarakby AA, Knight SF, et al. Obesity induced renal oxidative stress contributes to renal injury in salt-sensitive hypertension. *Clin Exp Pharmacol Physiol.* 2009;36(7):724–728.
47. Nistala R, Habibi J, Aroor A, et al. DPP4 inhibition attenuates filtration barrier injury and oxidant stress in the Zucker obese rat. *Obesity.* 2014;22(10):2172–2179.
48. Hayashi K, Kanda T, Homma K, et al. Altered renal microvascular response in Zucker obese rats. *Metabolism.* 2002;51(12):1553–1561.
49. Rothstein TL, Guo B. Receptor crosstalk: reprogramming B cell receptor signalling to an alternate pathway results in expression and secretion of the autoimmunity-associated cytokine, osteopontin. *J Intern Med.* 2009;265(6):632–643.
50. Nomiya T, Perez-Tilve D, Ogawa D, et al. Osteopontin mediates obesity-induced adipose tissue macrophage infiltration and insulin resistance in mice. *J Clin Invest.* 2007;117(10):2877–2888.
51. Fan W, Ankawi G, Zhang J, et al. Current understanding and future directions in the application of TIMP-2 and IGFBP7 in AKI clinical practice. *Clin Chem Lab Med.* 2019;57(5):567–576.
52. Su LJ, Li YM, Kellum JA, Peng ZY. Predictive value of cell cycle arrest biomarkers for cardiac surgery-associated acute kidney injury: a meta-analysis. *Br J Anaesth.* 2018;121(2):350–357.
53. Jia HM, Huang LF, Zheng Y, Li WX. Diagnostic value of urinary tissue inhibitor of metalloproteinase-2 and insulin-like growth factor binding protein 7 for acute kidney injury: a meta-analysis. *Crit Care.* 2017;21(1):77.
54. Stetler-Stevenson WG. Tissue inhibitors of metalloproteinases in cell signaling: metalloproteinase-independent biological activities. *Sci Signal.* 2008;1(27):re6.
55. Witzgall R, Brown D, Schwarz C, Bonventre JV. Localization of proliferating cell nuclear antigen, vimentin, c-Fos, and clusterin in the postischemic kidney. Evidence for a heterogeneous genetic response among nephron segments, and a large pool of mitotically active and dedifferentiated cells. *J Clin Invest.* 1994;93(5):2175–2188.
56. Katz N, Ronco C. Acute kidney stress: a useful term based on evolution in the understanding of acute kidney injury. *Crit Care.* 2016;20:23.
57. Hodgin JB, Nair V, Zhang H, et al. Identification of cross-species shared transcriptional networks of diabetic nephropathy in human and mouse glomeruli. *Diabetes.* 2013;62(1):299–308.